

Fundamental limits on the rate of bacterial cell division

Nathan M. Belliveau^{†, 1}, Griffin Chure^{†, 2, 3}, Christina L. Hueschen⁴, Hernan G. Garcia⁵, Jané Kondev⁶, Daniel S. Fisher⁷, Julie Theriot^{1, 8}, Rob Phillips^{2, 9, *}

*For correspondence:

[†]These authors contributed equally to this work

¹Department of Biology, University of Washington, Seattle, WA, USA; ²Division of Biology and Biological Engineering, California Institute of Technology, Pasadena, CA, USA; ³Department of Applied Physics, California Institute of Technology, Pasadena, CA, USA; ⁴Department of Chemical Engineering, Stanford University, Stanford, CA, USA; ⁵Department of Molecular Cell Biology and Department of Physics, University of California Berkeley, Berkeley, CA, USA; ⁶Department of Physics, Brandeis University, Waltham, MA, USA; ⁷Department of Applied Physics, Stanford University, Stanford, CA, USA; ⁸Allen Institute for Cell Science, Seattle, WA, USA; ⁹Department of Physics, California Institute of Technology, Pasadena, CA, USA; *Contributed equally

Abstract This will be written next

Protein synthesis

Lastly, we turn our attention to the process of translation. We begin by first estimating the number of tRNA synthetases and ribosomes required to double a cell in 5000 seconds. *E. coli* has roughly 3×10^6 proteins per cell, which for an average protein of 300 aa, amounts to the formation of $\approx 10^9$ peptide bonds. This value will also match the number of amino-acyl tRNA that are required for protein synthesis, with the pool of tRNA continuously recharging new amino acids by tRNA synthetases. At a rate of charging of about 20 amino-acyl tRNA per second (BNID: 105279, *Milo et al. (2010)*), we find that cells have more than sufficient tRNA synthetases to meet the ribosomal demand (*Figure 1(A)*). If we consider an elongation rate of ≈ 15 peptide bonds per second (BNID: 114271, *Milo et al. (2010); Dai et al. (2016)*), the formation of $\approx 10^9$ peptide bonds would require about 1.5×10^4 ribosomes. This is indeed consistent with the experimental data shown in *Figure 1(B)*.

So far our estimates have led to protein copy numbers that are consistent with the proteomic data, or even in excess of what might be needed for each task under limiting growth conditions. Even in our example of *E. coli* grown under different carbohydrate sources (??(B)), it becomes clear cells can utilize alternative carbon sources by inducing the expression of additional membrane transporters and enzymes. Optimal resource allocation and the role of ribosomal proteins have been an area of intense quantitative study over the last decade by Hwa and others (*Scott et al., 2010; Hui et al., 2015*). From the perspective of limiting growth, our earlier estimate of rRNA highlighted the necessity for multiple copies of rRNA genes in order to make enough rRNA. For *E. coli*'s fastest growth rates at 2 hr^{-1} , the additional demand for rRNA is further supported by parallelized DNA replication and increased rRNA gene dosage. This suggests the possibility that synthesis of ribosomes might be rate limiting. While the transcriptional demand for the ribosomal proteins is substantially lower than rRNA genes, since proteins can be translated from relatively fewer mRNA, other ribosomal proteins like the translation elongation factor EF-Tu also present a substantial burden. For EF-Tu in particular, it is the most highly expressed protein in *E. coli* and is

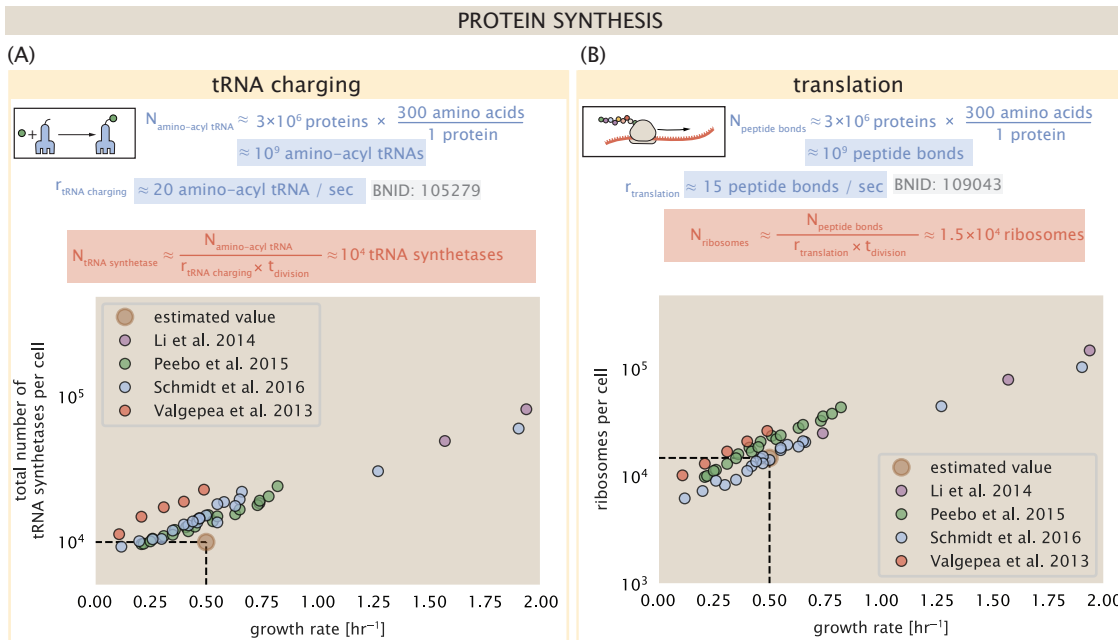


Figure 1. Estimation of the required tRNA synthetases and ribosomes. (A) Estimation for the number of tRNA synthetases that will supply the required amino acid demand. The sum of all tRNA synthetases copy numbers are plotted as a function of growth rate ([ArgS], [CysS], [GlnS], [GlxS], [IleS], [LeuS], [ValS], [AlaS]₂, [AsnS]₂, [AspS]₂, [TyrS]₂, [TrpS]₂, [ThrS]₂, [SerS]₂, [ProS]₂, [PheS]₂[PheT]₂, [MetG]₂, [lysS]₂, [HisS]₂, [GlyS]₂[GlyQ]₂). (B) Estimation of the number of ribosomes required to synthesize 10⁹ peptide bonds with an elongation rate of 15 peptide bonds per second. The average abundance of ribosomes is plotted as a function of growth rate. Our estimated values are shown for a growth rate of 0.5 hr⁻¹.

42 expressed from multiple gene copies, tufA and tufB.

43 To gain some intuition into how translation may set the speed limit for bacterial growth, we
44 again consider the total number of peptide bonds that must be synthesized, N_{AA} . Noting that cell
45 mass grows exponentially (**Godin et al., 2010**), we can compute the number of amino acids to be
46 polymerized as

$$N_{\text{AA}} = \frac{r_t R}{\lambda}, \quad (1)$$

47 where λ is the cell growth rate in s⁻¹, r_t is the maximum translation rate in amino acids per second,
48 and R is the average ribosome copy number per cell. Knowing the number of peptide bds to be
49 formed permits us to compute the translation-limited growth rate as

$$\lambda_{\text{translation-limited}} = \frac{r_t R}{N_{\text{AA}}}. \quad (2)$$

50 Alternatively, since N_{AA} is related to the total protein mass through the molecular weight of
51 each protein, we can also consider the growth rate in terms of the fraction of the total proteome
52 mass that is dedicated to ribosomal protein mass. By making the approximation that an average
53 amino acid has a molecular weight of 110 Da (see **Figure 2(A)**), we can rewrite the growth rate as,

$$\lambda_{\text{translation-limited}} \approx \frac{r_t}{L_R} \Phi_R, \quad (3)$$

54 where L_R is the total length in amino acids that make up a ribosome, and Φ_R is the ribosomal mass
55 fraction. This is plotted as a function of ribosomal fraction Φ_R in **Figure 2(A)**, where we take $L_R \approx$
56 7500 aa, corresponding to the length in amino acids for all ribosomal subunits of the 50S and 30S
57 complex (BNID: 101175, (**Milo et al., 2010**)). This formulation assumes that the cell can transcribe
58 the required amount of rRNA, which appears reasonable for *E. coli*, allowing us to consider the
59 inherent limit on growth set by the ribosome.

60 The growth rate defined by Equation 3 reflects mass-balance under steady-state growth and
61 has long provided a rationalization to the apparent linear increase in *E. coli*'s ribosomal content

as a function of growth rate (*Maaløe, 1979; Scott et al., 2010*). For our purposes, there are several important consequences of this trend. Firstly, we note there is a maximum growth rate of $\lambda \approx 6\text{hr}^{-1}$, or doubling time of about 7 minutes (dashed line). This growth rate can be viewed as an inherent maximum growth rate due to the need for the cell to double the cell's entire ribosomal mass. Interestingly, this limit is independent of the absolute number of ribosomes and is simply given by time to translate an entire ribosome, L_R/r_i . As shown in *Figure 2(B)*, we can reconcile this with the observation that in order to double the average number of ribosomes, each ribosome must produce a second ribosome. Unlike DNA replication or rRNA transcription, this is a process that cannot be parallelized.

For reasonable values of Φ_R , between about 0.1 - 0.3 (*Scott et al., 2010*), the maximum growth rate is in line with experimentally reported growth rates around 0.5 - 2 hr^{-1} . Importantly, in order for a cell to scale this growth limit they *must* increase their ribosomal abundance. This can be achieved by either synthesizing more ribosomes or reducing the fraction of non-ribosomal proteins. Reduction of non-ribosomal proteins is not a straightforward task since (as we have found throughout our estimates) doubling a cell requires many other enzymes and transporters. Increasing the absolute ribosomal abundance in *E. coli* will be limited by the number of rRNA operons.

Multiple replication forks help bias ribosome abundance.

E. coli cells grow by a so-called "adder" mechanism, whereby cells add a constant volume with each cell division (*Taheri-Araghi et al., 2015*). In conjunction with this, additional rounds of DNA replication are triggered when cells reach a critical volume per origin of replication (*Figure 3(A)*). This leads to the classically-described exponential increase in cell size with growth rate *Schaechter et al. (1958); Si et al. (2017, 2019)*. However, the mechanism behind growth rate control has remained elusive and has only been described at a phenomenological level. In the context of maximizing growth rate, it is notable that the majority of ribosomal proteins and rRNA operons are found closer to the DNA origin. Given that cells must increase their total gene dosage of rRNA operons at faster growth rates, and the intimate relationship between ribosomal content and growth rate considered above, this raises the possibility that the increase in chromosomal content might simply be a means for the cell to tune biosynthesis according to its physiological state and the nutrient availability in its environment.

While an increase in transcription has been observed for genes closer to the origin in rapidly growing *E. coli* (*Scholz et al., 2019*), we were unaware of such characterization at the proteomic level. In order to see whether there is a relative increase in protein expression for genes closer to the origin at faster growth, we calculated a running boxcar average (500 kbp window) of protein copy number as a function of each gene's transcriptional start site (*Figure 3(B)*). While absolute protein copy numbers can vary substantially across the chromosome, we indeed observe a bias in expression under fast growth conditions (dark blue), showing the result. The dramatic change in protein copy number near the origin is primarily due to the increase in ribosomal protein expression. This trend is in contrast to slower growth conditions (yellow) where the average copy number is more uniform across the length of the chromosome.

If ribosomal genes (rRNA and ribosomal proteins) are being synthesized at their maximal rate according to the rRNA gene dosage, we can make two related hypotheses about how their ribosome abundance should vary with chromosomal content. First, the ribosomal protein fraction should increase in proportion to the average ratio of DNA origins to DNA termini ($\langle \# \text{ ori} \rangle / \langle \# \text{ ter} \rangle$ ratio). This is a consequence of the skew in DNA dosage as cells grow faster. The second hypothesis is that the absolute number of ribosomes should increase with the number of DNA origins ($\langle \# \text{ ori} \rangle$), since this will reflect the total gene dosage at a particular growth condition.

In order to test each of these expectations we considered the experimental data from *Si et al. (2017)*, which inferred these parameters for cells under nutrient-limited growth. The ratio $\langle \# \text{ ori} \rangle / \langle \# \text{ ter} \rangle$ depends on how quickly chromosomes are replicated relative the cell's doubling time τ and

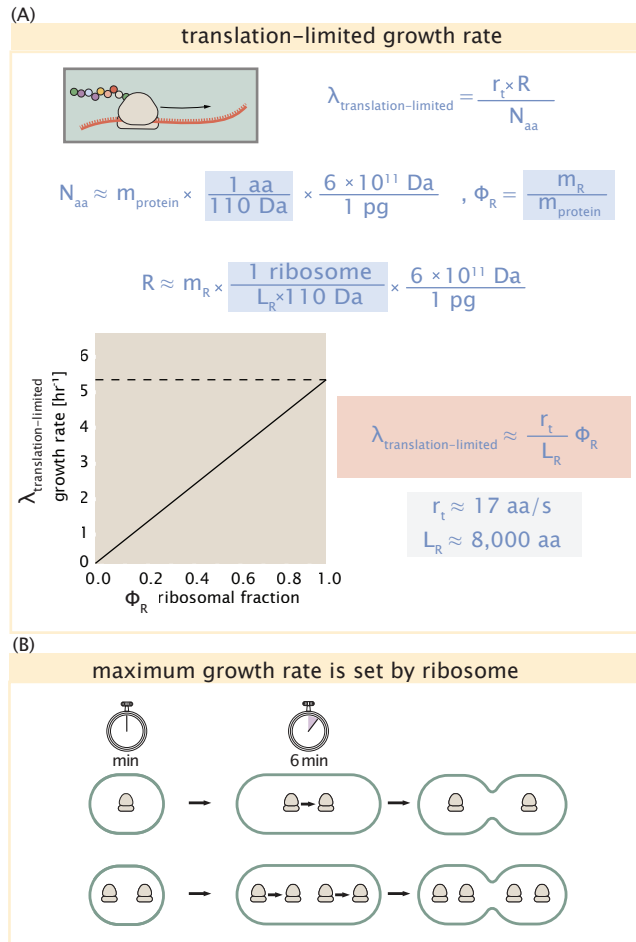


Figure 2. Translation-limited growth rate. (A) Here we consider the translation-limited growth as a function of ribosomal fraction. By mass balance, the time required to double the entire proteome (N_{AA} / r_t) sets the translation-limited growth rate, $\lambda_{\text{translation-limited}}$. Here N_{AA} is effectively the number of peptide bonds that must be translated, r_t is the translation elongation rate, and R is the number of ribosomes. This can also be re-written in terms of the ribosomal mass fraction $\Phi_R = m_R / m_{\text{protein}}$, where m_R is the total ribosomal mass and m_{protein} is the mass of all proteins in the cell. L_R refers to the summed length of the ribosomes in amino acids. $\lambda_{\text{translation-limited}}$ is plotted as a function of Φ_R (solid line). (B) The dashed line in part (A) identifies a maximum growth rate that is set by the ribosome. Specifically, this growth rate corresponds to the time required to translate an entire ribosome, L_R / r_t . This is a result that is independent of the number of ribosomes in the cell as shown schematically here.

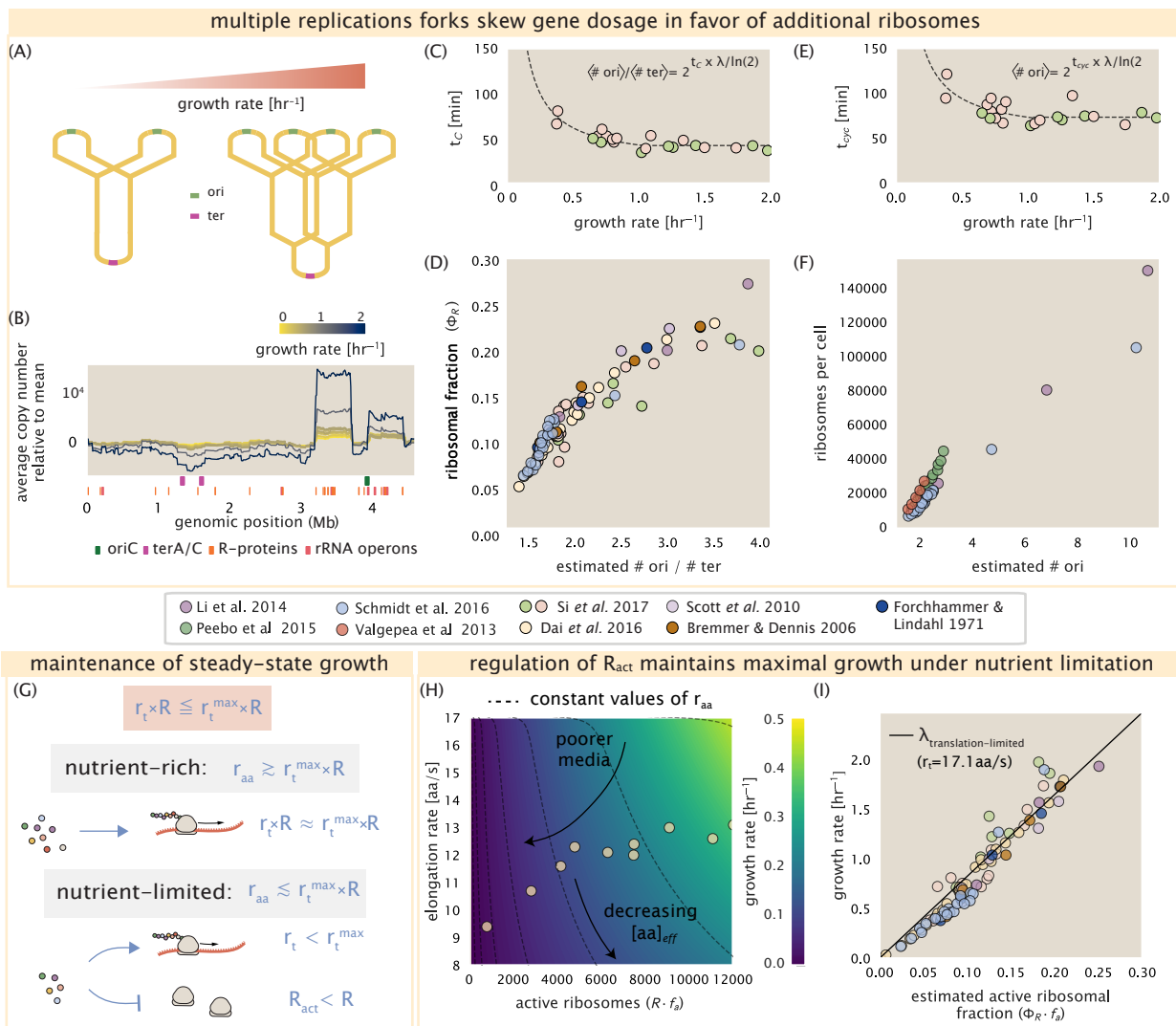


Figure 3. Multiple replication forks skew gene dosage and ribosomal content. (A) Schematic shows the expected increase in replication forks (or number of ori regions) as *E. coli* cells grow faster. (B) A running boxcar average of protein copy number is calculated for each growth condition considered by Schmidt *et al.*. A 0.5 Mb averaging window was used. Protein copy numbers are reported relative to their condition-specific means in order to center all data sets. (C) and (E) show experimental data from Si *et al.* (2017). Solid lines show fits to the data, which were used to estimate $\langle \# \text{ori} \rangle / \langle \# \text{ter} \rangle$ and $\langle \# \text{ori} \rangle$ [NB: to note fit equations]. Red data points correspond to measurements in strain MG1655, while light green points are for strain NCM3722. (D) Plot compares our estimate of $\langle \# \text{ori} \rangle / \langle \# \text{ter} \rangle$ to the experimental measurements of ribosomal abundance. Ribosomal fraction was approximated from the RNA/protein ratios of Dai *et al.* (2016) (yellow) and Si *et al.* (2017) (light red and light green) by the conversion RNA/protein ratio $\approx \Phi_R \cdot 2.1$. (F) Plot of the ribosome copy number estimated from the proteomic data against the estimated $\langle \# \text{ori} \rangle$. (G) Schematic showing translation-specific requirements for maintenance of steady-state growth. In a nutrient rich environment, amino acid supply r_{aa} is sufficiently in excess of the demand by ribosomes translating at their maximal rate. In poorer nutrient conditions, reduced amino acid supply r_{aa} will decrease the rate of elongation. In a regime where r_{aa} is less than $r_t \cdot R$, the number of actively translating ribosomes will need to be reduced in order to maintain steady-state growth. (H) Translation elongation rate is plotted as a function of the number of actively translating ribosomes $R \cdot f_a$. Dashed lines correspond to a range of amino acid synthesis rates r_{aa} , from 10^3 to 10^6 . Growth rates are calculated according to Equation 1, assuming a constant ribosomal fraction of 8 percent. See appendix XX for additional details. (I) Experimental data from Dai *et al.* are used to estimate the fraction of actively translating ribosomes. The solid line represents the translation-limited growth rate for ribosomes elongating at 17.1 AA/s.

112 is given by $2^{\tau_C/\tau}$. Here τ_C is the time taken to replicate *E. coli*'s chromosome, referred to as the C
 113 period of cell division. In **Figure 3(C)** we plot the measured τ_C versus τ (computed as $\tau = \log(2)/\lambda$),
 114 with data points in red corresponding to *E. coli* strain MG1655, and blue to strain NCM3722. **Si et al.**
 115 (2017) also measured the total RNA to protein ratio which reflects ribosomal abundance and we
 116 show that data along with other recent measurements from **Dai et al. (2016, 2018)**. Indeed, we
 117 find that the ribosomal fraction increases with $\langle \# \text{ ori} \rangle / \langle \# \text{ ter} \rangle$ (**Figure 3(C)**). We note a systematic
 118 difference in the relative abundances from **Peebo et al. (2015)** and **Valgepea et al. (2013)** that was
 119 inconsistent with a number of other measurements of total RNA-to-protein ratios ($\approx \Phi_R \times 2.1$ **Dai**
 120 **et al. (2016)**) and only show the data from **Schmidt et al. (2016)** and **Li et al. (2014)** for relative
 121 ribosome abundances (see supplemental section XX for a more complete discussion). For the data
 122 shown, the ribosomal fraction doesn't increase as much at higher $\langle \# \text{ ori} \rangle / \langle \# \text{ ter} \rangle$. Since several
 123 rRNA operons are actually located approximately half-way between the origin and terminus, the
 124 trend may in part be a consequence of a diminishing increase in rRNA gene dosage at higher $\langle \# \text{ ori} \rangle / \langle \# \text{ ter} \rangle$ ratios.
 125

126 We can similarly estimate $\langle \# \text{ ori} \rangle$, which depends on how often replication forks are initiated per
 127 cell cycle. This is given by the number of overlapping cell cycles, $2^{\tau_{\text{cyc}}/\tau}$, where τ_{cyc} refers to the total
 128 time of chromosome replication and cell division. **Figure 3(E)** shows the associated data from **Si**
 129 **et al. (2019)**, which we use to estimate $\langle \# \text{ ori} \rangle$ for each growth condition of the proteomic data. In
 130 agreement with our expectations, we find that ribosome copy number increases with the estimated
 131 $\langle \# \text{ ori} \rangle$ (**Figure 3(F)**).

132 While it is difficult to distinguish between causality and correlation, the data is at least consistent
 133 with the need for cells to increase their effective rRNA gene dosage in order to grow according to
 134 the constraint set by Equation 2. These results may also shed some light on the notable increase
 135 in ribosomal content that is observed when sublethal doses of antibiotics (**Scott et al., 2010; Dai**
 136 **et al., 2016**). Specifically, if rRNA synthesis is rate limiting, and nutrient conditions largely dictate the
 137 extent of overlapping DNA replication cycles, than addition of antibiotic will lengthen the doubling
 138 time and allow an increased rRNA synthesis relative to the rate of cell division. In Supplemental
 139 Section XX, we consider this further using additional data from **Si et al. (2017)**.

140 **Regulation of translating ribosomes helps maintain maximal growth according to
 141 nutrient availability.**

142 While the above analysis provides a possible explanation for how *E. coli* can vary its ribosomal
 143 content to maximize growth, it also presents a challenge in the limit of poorer nutrient conditions.
 144 Recall from Equation 3 that ribosomal content should decrease to zero as growth decreases to zero.
 145 While bacteria tend to decrease their ribosomal abundance in poorer nutrient conditions, they do
 146 so only to some fixed, non-zero amount (**Scott et al., 2010; Lieberman et al., 2014**). Here we find
 147 a minimal ribosomal fraction of ≈ 0.06 in the slowest growth conditions. From the perspective of a
 148 bacterium dealing with uncertain nutrient conditions, there is likely a benefit for the cell to maintain
 149 some relative fraction of ribosomes to support rapid growth as nutrient conditions improve.

150 The challenge however, lies in the cell's ability to maintain steady-state growth when ribosomes
 151 are in excess of the rate that nutrients can be harvested and amino acids synthesized for consump-
 152 tion **Figure 3G**. One explanation for this is that the elongation rate decreases in poorer growth
 153 conditions. Cells, however, are still able to maintain a relatively high elongation rate even in station-
 154 ary phase ($\approx 8 \text{ AA/s}$, (**Dai et al., 2016, 2018**)). A second explanation is that there are mechanisms
 155 to regulate biological activity in conditions of stress and nutrient-limitation; in particular through
 156 the small-molecule alarmones (p)ppGpp (**Harris and Theriot, 2018**). Here we explore these two
 157 observations to better understand their consequence on growth rate.

158 We consider slow growth conditions (λ less than 0.5 hr^{-1}) by assuming that the decrease in
 159 elongation rate is due to a limiting supply of amino acids and a need for the cell to maintain excess
 160 nutrients for cellular homeostasis under steady-state growth. There is some experimental support
 161 showing that in poorer nutrient growth conditions, cells have lower amino acids concentrations

162 (**Bennett et al., 2009**). We proceed by coarse graining the cell's amino acid supply as an single,
 163 effective rate-limiting species (see Supplemental Section XX for a more complete discussion). Under
 164 such a scenario, the elongation rate can described as simply depending on the maximum elongation
 165 rate (≈ 17.1 aa/s, (**Dai et al., 2016, 2018**)), an effective K_d , and the limiting amino acid concentration
 166 $[AA]_{eff}$. Specifically, the elongation rate is given by,

$$r_t = r_t^{max} \cdot \frac{1}{1 + K_d/[AA]_{eff}}. \quad (4)$$

167 For cells growing in minimal media + glucose, the amino acid concentration is of order 100 mM
 168 (BNID: 110093, (**Milo et al., 2010; Bennett et al., 2009**)). With a growth rate of about 0.6 hr^{-1} and
 169 elongation rate of 12.5 aa per second (**Dai et al., 2016**), we can estimate an effective K_d of about 40
 170 mM. Ultimately the steady state amino acid concentration will depend on the difference between
 171 the supply of amino acids r_{aa} and consumption by ribosomes $r_t \cdot R \cdot f_a$, where f_a accounts for the
 172 possible reduction of actively translating ribosomes.

173 In **Figure 3E** we consider how the maximal growth rate and elongation rates vary as a function of
 174 the number of actively translating ribosomes in this slow growth regime (see Supplemental Section
 175 XX for a complete description of the model). If we consider r_{AA} to be reflective of a specific growth
 176 condition, by considering lines of constant r_{AA} , we find that cells grow fastest by maximizing their
 177 fraction of actively translating ribosomes. When we consider the experimental measurements
 178 from **Dai et al. (2018)**, we see that although cells indeed reduce $R \times f_a$, they do so in a way that
 179 keeps $[AA]_{eff}$ relatively constant. Given our estimate for the K_d of 40 mM, we would only expect
 180 a decrease from 100 mM to about 35 mM in the slowest growth conditions. While experimental
 181 data is limited, amino acid concentrations only decrease to about 60 mM for cells grown in minimal
 182 media + acetate ($\lambda = 0.3\text{ hr}^{-1}$ in our proteomic data; value obtained from **Bennett et al. (2009)**),
 183 qualitatively consistent with our expectations.

184 Given the quantitative data from **Dai et al. (2018)**, which determined f_a across the entire range of
 185 growth rates across our data, we next estimated the active fraction of ribosomal protein. As shown
 186 in **Figure 3(G)**, we find that cells grow at a rate near the expected translation maximum expected
 187 from Equation 1, using the maximum elongation rate of $r_t = 17.1$ aa per second. This is in contrast
 188 to the reality that ribosomes are translating at almost half this rate in the poorest growth conditions.
 189 This highlights that there are alternative ways to grow according to the translated-limited growth
 190 rate that is expected based with ribosomes translating at their maximal elongation rate. Specifically,
 191 it is by adjusting $r_t \times R \times f_a \approx r_{max} \times R'$ that cells are able to scale the growth limit set by Equation 2.

192 [NB, These observations will be very important to include in discussion section: A number of
 193 recent papers highlight the possibility that (p)ppGpp may even provide a causal explanation for
 194 the nutrient-limit scaling law. In the context of ribosomal activity, increased levels of (p)ppGpp are
 195 associated with lower ribosomal content, and at slow growth appear to help reduce the fraction of ac-
 196 tively translating ribosomes (**Dai et al., 2016, 2018**). Titration of the cellular (p)ppGpp concetrations
 197 (up or down) can invoke similar proteomic changes reminiscent of those observed under nutrient
 198 limitation (**Zhu and Dai, 2019**). In light of the limiting dependence of ribosome copy number on
 199 chromosomal gene dosage, it was recently shown that growth in a (p)ppGpp null strain abolishes
 200 both the scaling in cell size and the $\langle \# \text{ ori} \rangle / \langle \# \text{ ter} \rangle$ ratio. Instead, cells exhibited a high $\langle \# \text{ ori} \rangle / \langle \# \text{ ter} \rangle$
 201 closer to 4 and cell size more consistent with a fast growth state where (p)ppGpp levels are low
 202 (**Fernández-Coll et al., 2020**).]

203 References

- 204 **Bennett BD**, Kimball EH, Gao M, Osterhout R, Van Dien SJ, Rabinowitz JD. Absolute metabolite concentrations
 205 and implied enzyme active site occupancy in *Escherichia coli*. *Nature Chemical Biology*. 2009 Aug; 5(8):593–599.
- 206 **Dai X**, Zhu M, Warren M, Balakrishnan R, Okano H, Williamson JR, Fredrick K, Hwa T. Slowdown of Translational
 207 Elongation in *Escherichia coli* under Hyperosmotic Stress. - PubMed - NCBI. *mBio*. 2018 Feb; 9(1):281.

- 208 **Dai X**, Zhu M, Warren M, Balakrishnan R, Patsalo V, Okano H, Williamson JR, Fredrick K, Wang YP, Hwa T. Reduction
209 of translating ribosomes enables *Escherichia coli* to maintain elongation rates during slow growth. *Nature Microbiology*. 2016 Dec; 2(2):16231.
- 211 **Fernández-Coll L**, Maciąg-Dorszynska M, Tailor K, Vadia S, Levin PA, Szalewska-Palasz A, Cashel M, Dunny GM.
212 The Absence of (p)ppGpp Renders Initiation of *Escherichia coli* Chromosomal DNA Synthesis Independent of
213 Growth Rates. *mBio*. 2020 Apr; 11(2):45.
- 214 **Godin M**, Delgado FF, Son S, Grover WH, Bryan AK, Tzur A, Jorgensen P, Payer K, Grossman AD, Kirschner
215 MW, Manalis SR. Using buoyant mass to measure the growth of single cells. *Nature Methods*. 2010 Apr;
216 7(5):387–390.
- 217 **Harris LK**, Theriot JA. Surface Area to Volume Ratio: A Natural Variable for Bacterial Morphogenesis. *Trends in
218 microbiology*. 2018 Oct; 26(10):815–832.
- 219 **Hui S**, Silverman JM, Chen SS, Erickson DW, Basan M, Wang J, Hwa T, Williamson JR. Quantitative proteomic
220 analysis reveals a simple strategy of global resource allocation in bacteria. *Molecular Systems Biology*. 2015
221 Feb; 11(2):e784–e784.
- 222 **Li GW**, Burkhardt D, Gross C, Weissman JS. Quantifying Absolute Protein Synthesis Rates Reveals Principles
223 Underlying Allocation of Cellular Resources. *Cell*. 2014 Apr; 157(3):624–635. doi: [10.1016/j.cell.2014.02.033](https://doi.org/10.1016/j.cell.2014.02.033).
- 224 **Liebermeister W**, Noor E, Flamholz A, Davidi D, Bernhardt J, Milo R. Visual account of protein investment in
225 cellular functions. *Proceedings of the National Academy of Sciences*. 2014 Jun; 111(23):8488–8493.
- 226 **MaaløeO**. Regulation of the Protein-Synthesizing Machinery—Ribosomes, tRNA, Factors, and So On. Goldberger
227 R, editor, *Gene Expression*, Springer; 1979.
- 228 **Milo R**, Jorgensen P, Moran U, Weber G, Springer M. BioNumbers—the Database of Key Numbers in Molecular
229 and Cell Biology. *Nucleic Acids Research*. 2010 Jan; 38(suppl_1):D750–D753. doi: [10.1093/nar/gkp889](https://doi.org/10.1093/nar/gkp889).
- 230 **Peebo K**, Valgepea K, Maser A, Nahku R, Adamberg K, Vilu R. Proteome Reallocation in *Escherichia coli* with
231 Increasing Specific Growth Rate. *Molecular BioSystems*. 2015; 11(4):1184–1193. doi: [10.1039/C4MB00721B](https://doi.org/10.1039/C4MB00721B).
- 232 **Schaechter M**, Maaløe O, Kjeldgaard NO. Dependency on Medium and Temperature of Cell Size and Chemical
233 Composition during Balanced Growth of *Salmonella typhimurium*. *Microbiology*. 1958 Dec; 19(3):592–606.
- 234 **Schmidt A**, Kochanowski K, Vedelaar S, Ahrné E, Volkmer B, Callipo L, Knoops K, Bauer M, Aebersold R, Heine-
235 man M. The Quantitative and Condition-Dependent *Escherichia coli* Proteome. *Nature Biotechnology*. 2016
236 Jan; 34(1):104–110. doi: [10.1038/nbt.3418](https://doi.org/10.1038/nbt.3418).
- 237 **Scholz SA**, Diao R, Wolfe MB, Fivenson EM, Lin XN, Freddolino PL. High-Resolution Mapping of the *Escherichia
238 coli* Chromosome Reveals Positions of High and Low Transcription. *Cell Systems*. 2019 Mar; 8(3):212–225.e9.
- 239 **Scott M**, Gunderson CW, Mateescu EM, Zhang Z, Hwa T. Interdependence of cell growth and gene expression:
240 origins and consequences. *Science*. 2010 Nov; 330(6007):1099–1102.
- 241 **Si F**, Le Treut G, Sauls JT, Vadia S, Levin PA, Jun S. Mechanistic Origin of Cell-Size Control and Homeostasis in
242 Bacteria. *Current Biology*. 2019 Jun; 29(11):1760–1770.e7. doi: [10.1016/j.cub.2019.04.062](https://doi.org/10.1016/j.cub.2019.04.062).
- 243 **Si F**, Li D, Cox SE, Sauls JT, Azizi O, Sou C, Schwartz AB, Erickstad MJ, Jun Y, Li X, Jun S. Invariance of Initiation Mass
244 and Predictability of Cell Size in *Escherichia coli*. *Current Biology*. 2017 May; 27(9):1278–1287.
- 245 **Taheri-Araghi S**, Bradde S, Sauls JT, Hill NS, Levin PA, Paulsson J, Vergassola M, Jun S. Cell-size control and
246 homeostasis in bacteria. - PubMed - NCBI. *Current Biology*. 2015 Feb; 25(3):385–391.
- 247 **Valgepea K**, Adamberg K, Seiman A, Vilu R. *Escherichia coli* Achieves Faster Growth by Increasing Catalytic and
248 Translation Rates of Proteins. *Molecular BioSystems*. 2013; 9(9):2344. doi: [10.1039/c3mb70119k](https://doi.org/10.1039/c3mb70119k).
- 249 **Zhu M**, Dai X. Growth suppression by altered (p)ppGpp levels results from non-optimal resource allocation in
250 *Escherichia coli*. *Nucleic Acids Research*. 2019 Mar; 47(9):4684–4693.